Evolution, 60(8), 2006, pp. 1537–1550

THE EVOLUTION OF GENETIC ARCHITECTURE UNDER FREQUENCY-DEPENDENT DISRUPTIVE SELECTION

MICHAEL KOPP[1,2] AND JOACHIM HERMISSON[1,3]
[1]*Section of Evolutionary Biology, Department of Biology II, Ludwig-Maximilian-University Munich, Großhadernerstraße 2, 82152 Martinsried, Germany*
[2]*E-mail: kopp@zi.biologie.uni-muenchen.de*
[3]*E-mail: hermisson@zi.biologie.uni-muenchen.de*

Abstract.—We propose a model to analyze a quantitative trait under frequency-dependent disruptive selection. Selection on the trait is a combination of stabilizing selection and intraspecific competition, where competition is maximal between individuals with equal phenotypes. In addition, there is a density-dependent component induced by population regulation. The trait is determined additively by a number of biallelic loci, which can have different effects on the trait value. In contrast to most previous models, we assume that the allelic effects at the loci can evolve due to epistatic interactions with the genetic background. Using a modifier approach, we derive analytical results under the assumption of weak selection and constant population size, and we investigate the full model by numerical simulations. We find that frequency-dependent disruptive selection favors the evolution of a highly asymmetric genetic architecture, where most of the genetic variation is concentrated on a small number of loci. We show that the evolution of genetic architecture can be understood in terms of the ecological niches created by competition. The phenotypic distribution of a population with an adapted genetic architecture closely matches this niche structure. Thus, evolution of the genetic architecture seems to be a plausible way for populations to adapt to regimes of frequency-dependent disruptive selection. As such, it should be seen as a potential evolutionary pathway to discrete polymorphisms and as a potential alternative to other evolutionary responses, such as the evolution of sexual dimorphism or assortative mating.

Key words.—Adaptive dynamics, epistasis, genetic variation, invasion fitness, modifier loci, quantitative genetics.

Received April 7, 2006. Accepted May 16, 2006.

Frequency-dependent disruptive selection is a form of selection that favors an increase in the phenotypic variance of quantitative traits. More precisely, the disruptive component favors extreme phenotypes, while the (negative) frequency-dependent component stabilizes the mean phenotype and maintains polymorphism (i.e., it prevents the whole population from evolving toward one phenotypic extreme). As a potential mechanism for genetic diversification, frequency-dependent disruptive selection has received considerable attention from evolutionary biologists. It is believed to play a prominent role in several important evolutionary processes, such as the maintenance of genetic variation (e.g., Bulmer 1974; Bürger and Gimelfarb 2004; Bürger 2005), the origin of sexual dimorphism (e.g., Bolnick and Doebeli 2003; van Dooren et al. 2004), or the evolution of reproductive isolation (e.g., Dieckmann and Doebeli 1999; Gavrilets 2004; Bolnick 2006).

Frequency-dependent disruptive selection arises naturally from a range of ecological scenarios. Widely studied examples include multiple-niche environments (Levene 1953; Kisdi and Geritz 1999a), sexual conflict (Gavrilets and Waxman 2002), predation (Abrams and Matsuda 1997; Doebeli and Dieckmann 2000), and intraspecific competition (Roughgarden 1972; Bulmer 1974; Brown and Vincent 1987; Dieckmann and Doebeli 1999; Bürger 2005; for empirical examples, see Swanson et al. 2003; Bolnick and Doebeli 2003; Bolnick 2004). These observations can be unified by the general framework of ''adaptive dynamics'' (e.g., Geritz et al. 1998). Adaptive dynamics models show that directional selection can move populations toward so-called evolutionary branching points, that is, areas in phenotype space where the mean phenotype corresponds to a stable fitness minimum (Abrams et al. 1993; Abrams and Matsuda 1997) and the population experiences frequency-dependent disruptive selection. In other words, population states characterized by frequency-dependent disruptive selection can be evolutionary attractors. In asexual populations, frequency-dependent disruptive selection can easily lead to the splitting of a previously homogeneous population into two or more subpopulations (hence the term ''evolutionary branching point''). In sexual populations, however, frequency-dependent disruptive selection favors genetic polymorphisms (e.g., Kisdi and Geritz 1999a; Bürger 2005), but under random mating, lineage splitting is prevented by segregation and recombination.

The phenotypic distribution that a sexually recombining population can maintain at equilibrium is constrained by the genetic architecture of the selected trait. The genetic architecture describes how the trait value is determined by the genotype (i.e., the genotype-phenotype map). In particular, it defines the number of loci that influence the trait and their relative effects. Over short time scales, the genetic architecture is constant, and selection can act only on allele frequencies within it. This is the assumption in the vast majority of population genetic models. In this case and under random mating, the constraints set by the genetic architecture will typically enforce a suboptimal phenotypic distribution. In particular, if all locus effects are equal and linkage is weak, the resulting phenotypic distribution is always unimodal. A bimodal (or multimodal) distribution can evolve only if additional options are built into the model. For example, Kisdi and Geritz (1999b) found that selection in spatially heterogeneous environments can reduce the migration rate between habitat patches. Bolnick and Doebeli (2003) and van Dooren et al. (2004) analyzed the evolution of sexual dimorphism at evolutionary branching points. Finally, Dieckmann and Doebeli (1999) and Doebeli and Dieckmann (2000), studying

models of competition, predation, and mutualism, found that frequency-dependent disruptive selection favors the evolution of assortative mating. The latter possibility has received considerable attention, because it is a potential way to sympatric speciation.

Over longer time scales, however, the genetic architecture of a quantitative trait can itself be subject to selection and evolutionary change (see Hermisson et al. 2003; Carter et al. 2005; reviewed by Hansen 2006). In this case, the need for more complicated adaptations, such as sexual dimorphism or assortative mating, may be reduced. For example, in a one-locus model, frequency-dependent disruptive selection was found to favor the evolution of dominance (van Dooren 1999). This increases the fitness of heterozygotes and makes mechanisms preventing matings between different homozygotes unnecessary. In general, however, evolution of the genetic architecture under frequency-dependent disruptive selection is still poorly understood.

Here, we use an explicit multilocus genetic model of a quantitative trait to study the evolution of the genetic architecture under frequency-dependent disruptive selection created by a combination of stabilizing selection and intraspecific competition. Making use of recent analytical results by Bürger (2005) and Bürger and Schneider (2006), we develop a modifier approach to investigate how epistatic interactions with the genetic background change the relative contribution of multiple loci to the trait value. We show that frequency-dependent disruptive selection leads to the evolution of a highly asymmetric genetic architecture, where most of the phenotypic variance is due to a small number of loci. The phenotypic distribution of the resulting population closely matches the set of ecological niches created by intraspecific competition.

The Model

Assumptions on Fitness

We consider a quantitative trait G that is subject to three sources of selection: stabilizing selection, frequency-dependent competition, and density-dependent population regulation. Our notation largely follows Bürger (2005).

Stabilizing selection is described by the Gaussian function

$$S(g) = \exp[-s(g - \theta)^2], \tag{1}$$

where g is the trait value or phenotype, θ is the optimal phenotype, and $s \geq 0$ determines the strength of stabilizing selection.

Competition between two individuals with phenotypes g and h similarly is described by the Gaussian function

$$\alpha(g, h) = \exp[-a(g - h)^2], \tag{2a}$$

where $a \geq 0$ determines the strength of selection due to competition. Competition is maximal for individuals with equal phenotype. For large a, only very similar individuals compete with each other. The average amount of competition experienced by an individual with phenotype g is

$$\bar{\alpha}_\pi(g) = \sum_h \alpha(g, h)\pi(h), \tag{2b}$$

where $\pi(h)$ is the frequency in the population of individuals with phenotype h. The index π in $\bar{\alpha}_\pi(g)$ stresses the fact that competition is frequency dependent. In the following, we will refer to the ratio

$$f = \frac{a}{s} \tag{3}$$

as the (relative) degree of frequency dependence.

Density-dependent population regulation acts according to a discrete logistic model. The growth rate of a phenotypically homogeneous population with $g = \theta$ and (total) size N is

$$F(N) = \rho - \frac{N}{\kappa}. \tag{4}$$

Here, ρ is the maximal population growth rate and κ is related to the carrying capacity K with

$$K = (\rho - 1)\kappa.$$

There are several ways to combine these fitness components into a single fitness function $W(g)$ (reviewed by Bürger 2005). In this paper, we use a model originally devised by Bulmer (1974) and an approximation derived by Bürger (2005). In the Bulmer model,

$$W(g) = F[N\bar{\alpha}_\pi(g)]S(g) = \left[\rho - \frac{N\bar{\alpha}_\pi(g)}{\kappa}\right]S(g). \tag{5}$$

Thus, there is a Lotka-Volterra type interaction between competition and density-dependent regulation: the fitness of an individual with genotype g is reduced by the presence of other individuals, but only as far as they are competitors. The product $N\bar{\alpha}_\pi(g)$ may be viewed as the ecologically effective population size experienced by the subpopulation with genotype g. Finally, stabilizing selection acts independently of density- and frequency-dependent selection (e.g., in different age classes).

If selection is weak, equation (5) can be approximated by the quadratic function

$$W(g) = \left(\rho - \frac{N}{\kappa}\right)\{1 - s(g - \theta)^2 + s\eta(N)[(g - \bar{g})^2 + V]\} \tag{6}$$

(Bürger 2005). Here, frequency dependence enters only through the mean phenotype $\bar{g}$ and the phenotypic variance V. The term

$$\eta(N) = f\frac{N}{\rho\kappa - N} \tag{7}$$

measures the strength of density- and frequency-dependent selection relative to stabilizing selection. If $\eta > 1$ (as we will assume throughout this paper) the fitness function is convex, meaning that the trait G is under frequency-dependent disruptive selection. As discussed in detail by Bürger (2005), η depends on the total population size N. If $N = K$ then $\eta(N) = f(\rho - 1)$. In this paper, we usually assumed $\rho = 2$. Furthermore, the total size of a polymorphic populations was typically greater than K (see Fig. 8 below). Therefore, $\eta > 1$ whenever $f > 1$.

Assumptions on Genetics

We consider a population with equivalent sexes, random mating, and discrete generations. Population size is suffi-

ciently large to ignore genetic drift in resident genotypes. Genetics can be either haploid or diploid.

Primary loci

The trait G is determined additively by n biallelic loci (henceforth referred to as primary loci) with alleles A_i and a_i. In haploids, the contribution of locus i to the phenotype g is γ_i for individuals carrying the A_i allele and $-\gamma_i$ for individuals carrying the a_i allele. In diploids, these contributions are γ_i for A_iA_i homozygotes, zero for A_ia_i heterozygotes, and $-\gamma_i$ for a_ia_i homozygotes ($\gamma_i \geq 0$). Note that, because we neglect environmental influences on the trait, we equate genotypic value and phenotypic value. At any point in time, loci are labeled (and, if necessary, relabeled) such that

$$\gamma_1 \leq \gamma_2 \leq \ldots \leq \gamma_n. \tag{8}$$

Furthermore, we define

$$\Gamma \equiv \sum_{i=1}^{n} \gamma_i \tag{9}$$

and refer to the interval from $-\Gamma$ to Γ as the phenotypic range of the trait. We assume that the phenotype favored by stabilizing selection, θ, is within the phenotypic range.

The γ_i are the locus mutational effects or simply ''locus effects''. Loci with small or large effects will be referred to as ''weak'' or ''strong'' loci, respectively. A single strong locus that covers almost the whole phenotypic range is called a ''major locus.''

Modifier loci

We define the vector of locus effects $\boldsymbol{\gamma} = (\gamma_1 \ldots \gamma_n)^T$ (where T denotes transposition) as the genetic architecture of the trait G. This follows the suggestion by Wagner et al. (1997) to measure genetic architecture in terms of mutational effects. In the following, a genetic architecture with equal or similar locus effects will be called ''symmetric'' and a genetic architecture with largely unequal locus effects ''asymmetric.''

The aim of this paper is to study the evolution of the genetic architecture $\boldsymbol{\gamma}$. For this purpose, we assume that the effects of the primary loci, that is, the γ_i, are influenced by modifier loci, and we analyze evolution at these modifier loci. The use of modifiers is a standard way of performing invasion analysis (see below) in a population genetics context. In contrast to the primary loci, the modifier loci support a continuum of possible alleles. In the diploid case, the two alleles per modifier locus determine the effect of the primary locus additively. Note that, in our approach, the evolution of genetic architecture is symmetric, in the sense that the phenotypic contributions of the A_i and a_i alleles always have the same absolute value. In the diploid model, this means that the phenotypic contribution of heterozygous (primary) loci is always zero, as we do not allow for evolution of dominance (van Dooren 1999).

In the following, we investigate evolution at the modifier loci both analytically and numerically. Our analytical approach is based on the methodology of adaptive dynamics (e.g., Geritz et al. 1998), that is, it focuses on the fitness of invading mutants. For the numerical analysis, we use deterministic simulations of haplotype frequencies, coupled with a stochastic model for the extinction and creation of modifier alleles. Details of the simulation methods are given in Appendix 2 (available online only at http://dx.doi.org/10.1554/06-220.1.s1). We first study the weak-selection approximation (6), and then go on to investigate the full model (5) with strong selection.

Results

The Weak-Selection Approximation

In the following, we will use fitness function (6) and make the simplifying assumptions that all loci are at linkage equilibrium and population size is constant (e.g., at the demographic equilibrium; cf. Bürger 2005) We therefore can treat $\eta(N) \equiv \eta$ as a constant. Under these assumptions, the evolutionary equilibrium of the primary loci with a fixed genetic architecture (i.e., for monomorphic modifier loci) has recently been derived by Bürger (2005) and Bürger and Schneider (2006). Briefly, for $\eta > 1$, there is a unique equilibrium where the weakest loci may be monomorphic, but at least one locus is always polymorphic. If the number of monomorphic loci is m (with $0 \leq m < n$), then there is a quantity Θ_m that separates monomorphic and polymorphic loci, such that

$$\gamma_i \leq |\Theta_m| \quad \text{for } 1 < i \leq m \text{ (monomorphic loci)} \tag{10a}$$

and

$$\gamma_i > |\Theta_m| \quad \text{for } m < i \leq n \text{ (polymorphic loci).} \tag{10b}$$

More details, including the value of Θ_m and the equilibrium allele frequencies, are given in Appendix 1. Using these results, it is possible to obtain analytical results for the evolution of $\boldsymbol{\gamma}$.

We focus on the fitness of a rare mutant modifier allele which changes γ_i to $\gamma_i + \Delta\gamma_i$, where $\Delta\gamma_i$ is called the mutational increment. In the diploid case, we must specify that $\Delta\gamma_i$ is the effect of a single copy of the mutant allele. We make the standard assumptions that the mutational increment is small and mutations enter the population one at a time (i.e., rarely), such that, when a new mutation arises, the resident population is monomorphic at the modifier loci and the allele frequencies at the primary loci are at equilibrium. Our goal is to calculate the fitness increment due to the mutation, $\Delta\bar{W}^*$, which is the difference in the mean fitness of mutants and residents while the mutants are rare. Only mutants with a positive fitness increment have a chance to invade the population and eventually go to fixation.

Evolution of a single locus effect

We first investigate the evolution of the effect γ_i of a single locus i. For small mutations, the fitness increment can be approximated to first order by

$$\Delta\bar{W}^* \approx \Delta\gamma_i \left.\frac{\partial\bar{W}^*}{\partial\gamma_i^*}\right|_{\gamma_i^*=\gamma_i}, \tag{11}$$

where the asterisk indicates parameters of mutant individuals. The derivative in equation (11) is the selection gradient (or invasion fitness gradient) with respect to the locus effect γ_i.

In Appendix 1, we show that the selection gradient is given by

$$\frac{\partial \bar{W}^*}{\partial \gamma_i^*} = \begin{cases} 2s(\eta - 1)Q_i & \text{in the haploid case} \\ s(\eta - 1)Q_i & \text{in the diploid case,} \end{cases} \tag{12a}$$

where

$$Q_i = \begin{cases} |\Theta_m| & \text{for monomorphic loci } (i \leq m) \\ \gamma_i & \text{for polymorphic loci } (i > m). \end{cases} \tag{12b}$$

Thus, for polymorphic loci, the selection gradient is proportional to the resident locus effect γ_i. In other words, the modifiers are under (quadratic) directional selection of strength $2s(\eta - 1)$. For all monomorphic loci, the selection gradients are identical and equal to those of a locus at the brink of becoming polymorphic (see eq. 10). In particular, the selection gradient for monomorphic loci is always weaker than for polymorphic loci. Inserting equation (12) into equation (11) shows that the effect of the locus can only increase (the fitness increment is positive only for positive mutational increments). Furthermore, because the selection gradient is predicted to be proportional to the speed of evolution, the locus effect should increase at an accelerating rate.

Evolution of multiple locus effects

Next, we generalize the results of the previous section by considering a mutation at a modifier locus that simultaneously changes the effects of several primary loci. We write that the mutation changes $\boldsymbol{\gamma} \mapsto \boldsymbol{\gamma} + \Delta\boldsymbol{\gamma}$, that is

$$\begin{aligned} \gamma_1 &\mapsto \gamma_1 + \Delta\gamma_1 \\ &\vdots \\ \gamma_n &\mapsto \gamma_n + \Delta\gamma_n. \end{aligned} \tag{13}$$

$\Delta\boldsymbol{\gamma}$ is the vector of mutational increments, with the per locus mutational increments $\Delta\gamma_i$ as components.

In analogy to equation (11), the fitness increment due to the mutation can now be approximated by

$$\Delta\bar{W}^* \approx \sum_i \Delta\gamma_i \left.\frac{\partial \bar{W}^*}{\partial \gamma_i^*}\right|_{\boldsymbol{\gamma}^* = \boldsymbol{\gamma}}. \tag{14}$$

Applying equation (12), this evaluates to

$$\Delta\bar{W}^* = \begin{cases} 2s(\eta - 1)\tilde{Q} & \text{in the haploid case} \\ s(\eta - 1)\tilde{Q} & \text{in the diploid case,} \end{cases} \tag{15a}$$

with

$$\tilde{Q} = \sum_{i=1}^{n} Q_i \Delta\gamma_i = |\Theta_m| \sum_{i \leq m} \Delta\gamma_i + \sum_{i > m} \gamma_i \Delta\gamma_i. \tag{15b}$$

Invasion of the mutant is possible if and only if $\tilde{Q} > 0$. This term is a weighted mean of the per locus mutational increments $\Delta\gamma_i$, with the weights being proportional to Q_i. Thus, a mutation that increases the effects of some loci but decreases those of other loci can only invade if the weighted mean increase in the effects of the first group of loci is greater than the weighted mean decrease in the effects of the second group. As the weight of a locus increases with its current effect (eq. 12b), this is most likely if the loci having their effect increased are those that are already strongest. Therefore, the genetic architecture should become more and more asymmetric, while the phenotypic range of the trait increases. For the case with symmetric stabilizing selection ($\theta = 0$), this means that the phenotypic variance of the population always increases (see Appendix 1).

Constrained phenotypic range

The predictions from the previous section clearly cannot hold true forever. The evolution of ever more diverging phenotypes is bound to eventually come to a halt, either by direct constraints on the range of feasible phenotypes or by reduced fitness of extreme phenotypes. In the following, we investigate the first possibility, constrained phenotypic range. The second case will be dealt with in the next section.

We will assume a constraint on Γ, the sum of the locus effects γ_i. The basic idea is that an increase in the effect of one locus is not possible without a compensatory decrease in the effects of one or more other loci. For example, the primary loci might be viewed as coding for enzymes contributing to a common metabolic pathway and competing for a limited resource. Then equation (15) shows that strong loci are more likely to evolve an increased effect than weak loci, because they are under a stronger selection pressure (i.e., their selection gradient is steeper).

As a specific example, assume a mutation increasing the effect of locus k and decreasing the effects of all other loci. Let the mutational increments be

$$\Delta\gamma_i = \begin{cases} \left[1 - \dfrac{\gamma_i}{\Gamma} y(\Gamma)\right] \tilde{\Delta}\gamma_k & \text{for } i = k \\ -\dfrac{\gamma_i}{\Gamma} y(\Gamma) \tilde{\Delta}\gamma_k & \text{for } i \neq k, \end{cases} \tag{16a}$$

where $y(\Gamma)$ is a function satisfying

$$y(0) = 0, \tag{16b}$$

$$y'(\Gamma) > 0, \tag{16c}$$

$$\lim_{\Gamma \to \Gamma_{\max}} y(\Gamma) = 1. \tag{16d}$$

Basically, this means that, after an hypothetical initial increase $\tilde{\Delta}\gamma_k$ of γ_k, a total proportion $y(\Gamma)$ of $\tilde{\Delta}\gamma_k$ is subtracted from all loci (including locus k), with the deduction proportional to the current locus effects. The properties of the function $y(\Gamma)$ guarantee that Γ asymptotically approaches a maximum value $\Gamma_{\max}$. Inserting (16) into (15) yields

$$\Delta\bar{W}^* = \frac{y(\Gamma)\tilde{\Delta}_{\gamma_k}}{\Gamma}\left[Q_k \frac{\Gamma}{y(\Gamma)} - \tilde{Q}_c\right] \quad \text{with} \tag{17a}$$

$$\tilde{Q}_c = \sum_{i=1}^{n} Q_i \gamma_i = |\Theta_m| \sum_{i \leq m} \gamma_i + \sum_{i > m} \gamma_i^2. \tag{17b}$$

Therefore, a mutation increasing γ_k (i.e., with $\Delta\gamma_k > 0$) can invade if and only if

$$Q_k \Gamma > y(\Gamma)\tilde{Q}_c. \tag{18}$$

As long as $y(\Gamma)$ is close to zero, many mutants with positive mutational increment can invade. As Γ approaches $\Gamma_{\max}$, the trade-off between locus effects is maximal and every increase in the effect of one locus must be compensated by decreases

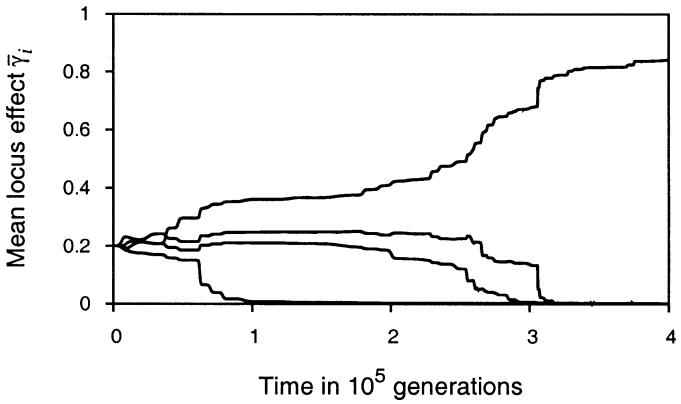

FIG. 1. Evolution of the genetic architecture under the weak-selection approximation (eq. 6) with constrained phenotypic range and free recombination. The figure shows the mean effects $\bar{\gamma}_i$ of four haploid loci over time in an exemplary simulation run. The initial genetic architecture was symmetric but evolved to an asymmetric state characterized by a single major locus. Note that the maximal locus effect was $\Gamma_{max} = 1$, but the simulation was stopped once the effect of the strongest locus had reached the value of 0.8. Parameters: $a = 0.2$, $s = 0.02$, $r = 0.5$, $\kappa = 10000$, $\rho = 2$, $\theta = 0$. See online Appendix 2 for further details.

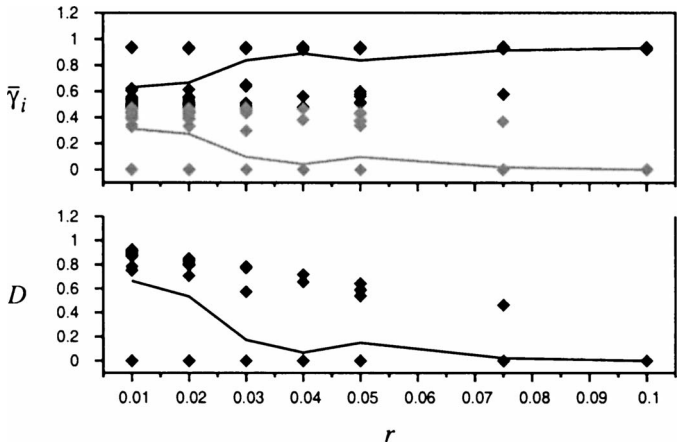

FIG. 2. The effects of linkage on the evolution of the genetic architecture under the weak-selection approximation (eq. 6) with constrained phenotypic range. The top panel shows the mean locus effects $\bar{\gamma}_i$ after 2×10^6 generations in a haploid two-locus model as a function of r, the recombination rate between adjacent loci. Diamonds show the results of 20 replicated simulations, and lines are the means over these 20 replicates. For each replicate, the locus with the larger effect is marked in black and the one with the smaller effect in gray. The second panel shows D, a measure of global linkage disequilibrium. D is defined as $(V - V_{LE})/V_{LE}$, where V is the actual phenotypic variance and V_{LE} the variance assuming linkage equilibrium. That is, D is the relative increase of phenotypic variance due to linkage disequilibrium. There are two main outcomes of the simulations. Either the two loci have similar effects and D is high, or both the effect of the second locus and D are close to zero. The proportion of simulations showing the first outcome decreases with r. Parameters: $s = 0.02$, $a = 0.2$, $\theta = 0$, $\rho = 2$, $\kappa = 10000$. See online Appendix 2 for further details.

in the effects of the other loci. In the limit of $\Gamma \to \Gamma_{max}$, equation (18) leads to the following conclusions (Appendix 1): (1) the effect of the strongest locus (i.e., locus n) will always increase further; (2) if all loci are polymorphic the effect of the weakest locus will always decrease further; (3) if the m weakest loci are monomorphic, all of their effects will decrease further; and (4) if there are no other constraints on the genetic architecture, the outcome of evolution of $\boldsymbol{\gamma}$ is one polymorphic locus with maximal effect, which accumulates all genetic variation, while the effects of all other loci go to zero—that is, evolution of a single major locus.

These conclusions were confirmed by numerical simulations. In the simulations, we relaxed several assumptions of the invasion analysis (see online Appendix 2). In particular, population size was not held constant, the primary loci were not assumed to be at equilibrium, mutations with positive invasion fitness did not automatically go to fixation, and more than one modifier locus was allowed to be polymorphic at the same time. Also, we tested various degrees of linkage among loci. For almost all parameter combinations and initial conditions tested, the population evolved toward a state where only one locus had an effect significantly different from zero, and the effect of this locus approached the maximal effect Γ_{max} (Fig. 1; due to the asymptotic nature of $y(\Gamma)$, this approach is rather slow). The only exceptions occurred when the recombination rate was very low ($r < 0.1$ between adjacent loci). In these cases, two or more loci maintained a significant effect (with the combined effect being close to Γ_{max}) while building up strong linkage disequilibrium. Both the amount of linkage disequilibrium and the proportion of simulations showing this result decreased with increasing r (Fig. 2).

The above results can be easily understood by noting that, within the realm of the weak-selection approximation, selection is always purely disruptive (because eq. 6 is a quadratic function of phenotype g). In other words, the most extreme phenotypes always have the highest fitness. As illustrated in Figure 3, a genetic architecture with a single major locus maximizes the frequency of extreme phenotypes and minimizes the frequency of intermediate ones. In the haploid case, only the extreme phenotypes coexist. In the diploid case, individuals that are heterozygous at the major locus have intermediate phenotypes and suffer reduced fitness, which is unavoidable in the absence of dominance. Even in this case, however, the frequency of intermediate phenotypes is minimized by a genetic architecture with a single major locus.

The Full Model with Strong Selection

The weak-selection approximation, and therefore the assumption of purely disruptive selection, is justified only if the phenotypic range of the species under study is small relative to the width of the stabilizing selection function. This was true in the previous analysis because the phenotypic range was subject to a direct constraint. Without such a constraint, the fitness of extreme phenotypes will eventually be reduced by stabilizing selection. If this happens, the weak-selection approximation breaks down, and we must instead investigate the full model given by equation (5).

Asexual reproduction

To better understand the consequences of strong selection, it is highly instructive to first study evolution in a population

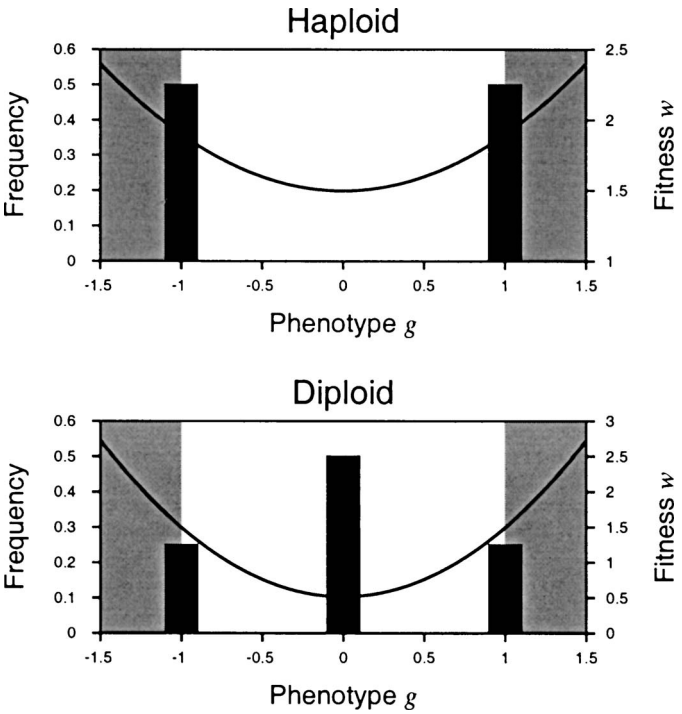

FIG. 3. Phenotypic distributions and frequency-dependent fitness functions under the weak-selection approximation (eq. 6) with constrained phenotypic range. The plots show the state of a polymorphic population with one major locus ($p_i = 0.5$ for all i; $\gamma_i = 0$ for $i < n$, $\gamma_n = \Gamma_{max} = 1$). The nonshaded area is the phenotypic range. Selection is purely disruptive, and extreme phenotypes have the highest fitness.

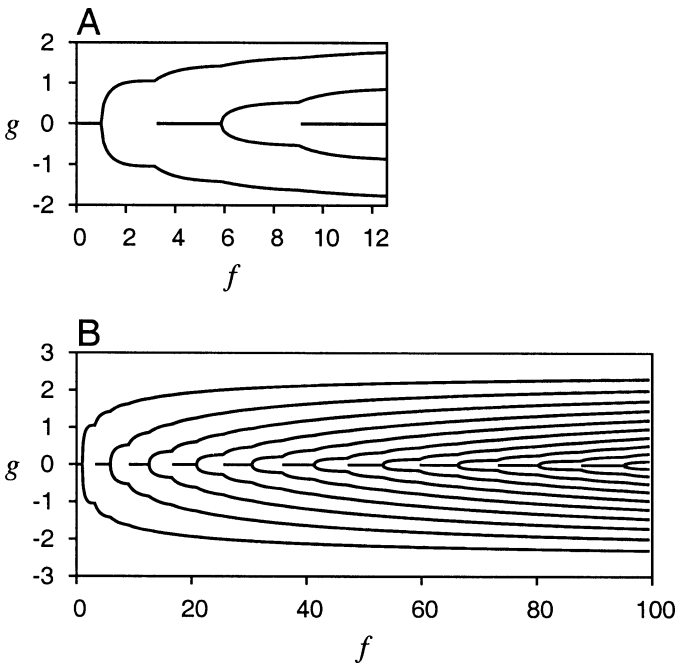

FIG. 4. Equilibrium phenotypic distributions in an asexual version of the full model (eq. 5) as a function of f, the degree of frequency dependence (assuming $\rho = 2$ and $s = 0.1$). The two panels differ only in the range of f-values shown, with the upper panel giving a detailed view for $f \leq 12.6$.

with asexual (i.e., clonal) reproduction. Because such a population is free of genetic constraints (e.g., due to recombination), its equilibrium phenotypic distribution can be regarded as optimal. Below, we will compare this optimal distribution with the phenotypic distribution reached in a sexual population.

The exact equilibrium distribution in the asexual model can be computed numerically without resorting to simulations (see Appendix 3, available online only at http://dx.doi.org/10.1554/06-220.1.s1). The results are shown in Figure 4. Most notably, the number of coexisting phenotypes increases with the degree of frequency dependence, f. For $f < 1$, only one phenotype can exist, which is equal to the optimal phenotype θ. At $f = 1$, this phenotype is replaced by two phenotypes, which at $f = 3.26$ can be invaded by a third, intermediate phenotype, which at $f = 5.96$ itself branches into two phenotypes, and so on. The phenotypes in Figure 4 can be viewed as occupying discrete ecological niches (with the niche width being inversely proportional to f), which arise from the combination of competition and stabilizing selection (cf. Roughgarden 1972; Ackermann and Doebeli 2004; Bolnick 2006).

Sexual reproduction

We now return to the genetically explicit sexual model, which can only be studied by simulations. The main result of these simulations is that the genetic architecture evolves in such a way that the phenotypic distribution of a sexually recombining population closely matches the niche structure predicted by the asexual model (Fig. 4).

The basic principles can be learned from the simplest case, that of a haploid population with symmetric stabilizing selection ($\theta = 0$) and free recombination ($r = 0.5$; simulations with asymmetric stabilizing selection and linkage are described in Appendix 4, which is available online only at http://dx.doi.org/10.1554/06-220.1.s1). As shown in Figure 5, the number of coexisting phenotypes increases with the degree of frequency dependence, f, and is at least close to the number of phenotypes predicted in Figure 4. Figure 5 also shows the genetic architectures underlying these phenotypic distributions. In all examples shown here, the primary loci were polymorphic with allele frequencies equal to $p_i = 0.5$. For $f = 2$, the two coexisting phenotypes are determined by a single major locus. Thus, the genetic architecture is the same as under the weak-selection approximation. For larger f, however, the genetic architecture becomes more complex, which allows for the coexistence of more than two phenotypes. In particular, there are two major trends: (1) the modifier loci may be polymorphic, meaning that locus effects differ between individuals (note that, in the simulations, we assumed that there is one modifier locus per primary locus; see online Appendix 2), and (2) more than one locus can contribute to the phenotype (i.e., have a mean effect significantly different from zero).

Both mechanisms can be seen for $f = 5$, where they lead to two alternative outcomes. In the first simulation (a in Fig. 5), a single primary locus determines the phenotype, but the corresponding modifier locus is polymorphic. That is, the

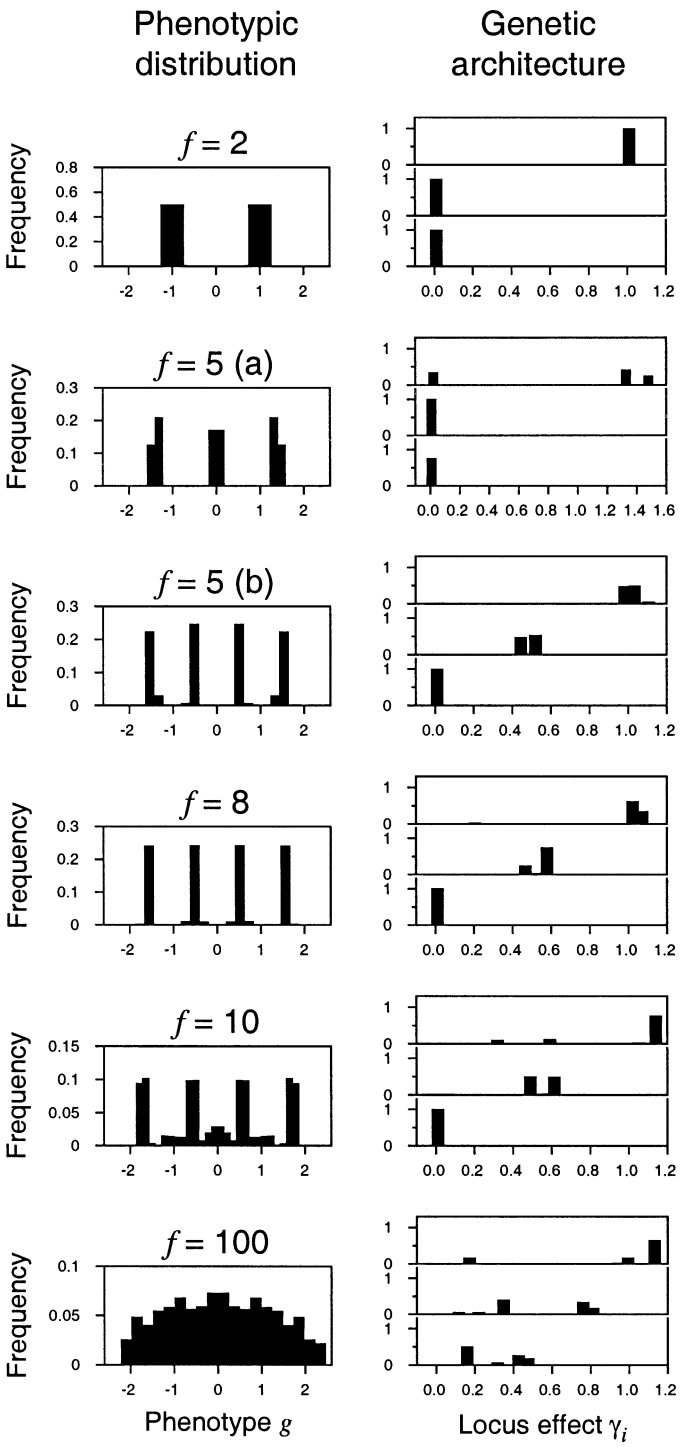

FIG. 5. Phenotypic distributions and genetic architectures evolving in the full model (eq. 5). The figures show the results of typical simulation runs after 10^5 generations in a haploid, three-locus model with symmetric stabilizing selection ($\theta = 0$) and free recombination ($r = 0.5$) for various degrees of frequency dependence, f (assuming $s = 0.1$). For $f = 5$, two simulations are shown, which led to alternative outcomes. The histograms on the left side show the phenotypic distributions, that is, the frequencies of 30 classes of phenotypes. The numbers of coexisting phenotypes predicted by the asexual model (Fig. 4) were two for $f = 2$, three for $f = 5$, four for $f = 8$, five for $f = 10$, and 20 for $f = 100$. The panels on the right side show the underlying genetic architectures, that is, the distributions of locus effects γ_i, as determined by the corresponding modifier loci. Each panel shows the values and frequencies of alleles at one modifier locus, and loci are ordered according to their mean effects $\bar{\gamma}_i$. The number of coexisting alleles per modifier locus was limited to $k = 6$. In the simulations shown here, the primary loci were always polymorphic with allele frequencies $p_i = 0.5$. As predicted by the asexual model (Fig. 4), the number of coexisting phenotypes increases with f. This is achieved by increasing the number of loci contributing to the phenotype (i.e., the number of of loci with an effect significantly different from zero). The resulting genetic architecture is always asymmetric. Furthermore, numbers of phenotypes not equal to a power of 2 require polymorphism at the modifier loci ($f = 5$ [a], $f = 10$, $f = 100$).

effect of the primary locus is large only in some individuals (those with the extreme phenotypes) but close to zero in others (those with the intermediate phenotype). The resulting distribution of three phenotypes matches the one predicted by the asexual model. In the second simulation (b in Fig. 5), the phenotype is determined by two primary loci with monomorphic modifiers, where the effect of the first locus is about twice that of the second one. With polymorphic primary loci, such an asymmetric genetic architecture leads to four coexisting phenotypes with nearly equal distances between them. Although this distribution would not be stable in the asexual model (because the intermediate phenotypes have reduced fitness), in the sexual model, it is maintained by a balance between selection and recombination. The same distribution is also reached for $f = 8$ (where it is in accordance with the asexual model). For larger f, the two mechanisms, polymorphic modifiers and multiple loci with a positive effect, may be combined. In the example shown for $f = 10$, two primary loci contribute to the phenotype, and one of the modifier loci is polymorphic, leading to a distribution of five phenotypic clusters (as predicted by the asexual model). In the extreme case of $f = 100$, all three primary loci contribute to the phenotype, all modifier loci are polymorphic, and the resulting phenotypic distribution is nearly continuous.

For small f, only one or two primary loci contribute to mean phenotype and to the phenotypic variance. The other loci evolve an effect close to zero, that is, they become essentially neutral (even though the primary loci typically stay polymorphic). In some simulations, we observed an alternative outcome that leads to a similar result: instead of loci loosing their effect, two or more loci with a positive effect became fixed for one of their alleles, and the combined contribution of these loci to the phenotype was close to zero (or, more generally, to θ). The likelihood of this outcome depends on initial conditions—it appears to be most likely if the the locus effects are high already at the beginning of a simulation—but for most parameter combinations, it is the exception rather than the rule. In both cases, the genetic architecture is identical with respect to those loci that contribute to the phenotypic variance (and can be detected by quantitative trait loci methods). In Figures 6 and 7 (see below), we will ignore monomorphic loci and only show the effects of polymorphic loci (even if they are zero).

Figure 6 provides a systematic overview of how the genetic architecture depends on f and on the total number of loci, n. It reveals two major trends. First, the degree of polymorphism at the modifier loci (measured as the total variance of locus

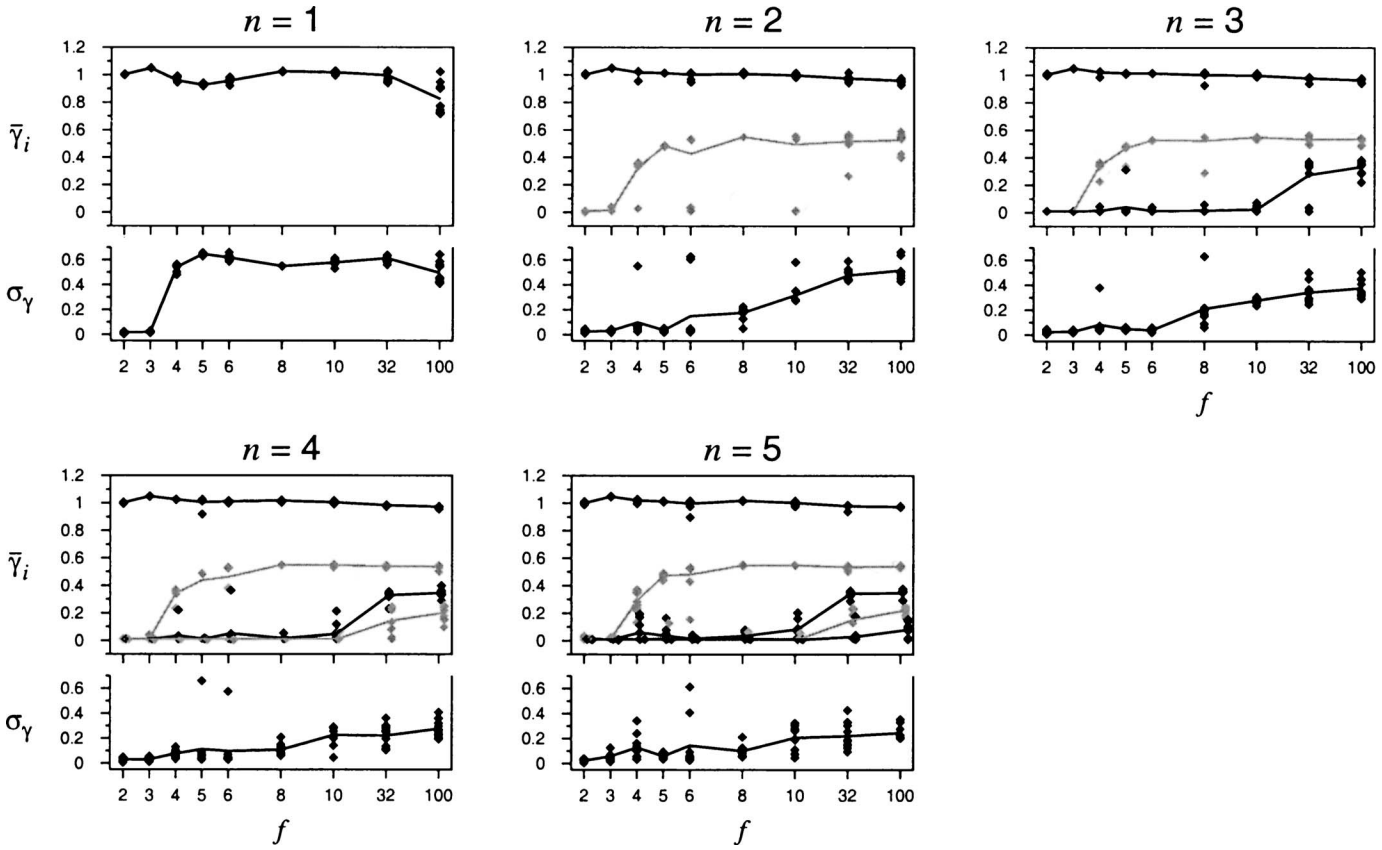

FIG. 6. The genetic architecture evolving in the haploid full model (eq. 5) as a function of f, the degree of frequency dependence, for various numbers of primary loci, n. The figures show the results of 10 replicated simulations per parameter combination in a model with symmetric stabilizing selection ($\theta = 0$) and free recombination ($r = 0.5$). Dots represent results of individual simulations and lines are the means over the 10 replicates. For each n, the top panel shows the mean effect of each primary locus $\bar{\gamma}_i$. In most cases, the primary loci themselves where polymorphic with allele frequencies $p_i = 0.5$. Effects of monomorphic primary loci are not shown. The loci are ordered according to their mean effects, and black and gray indicate loci with alternating positions in this order. The bottom panels show the square-root of the total variance of locus effects, σ_γ, which is a measure for the degree of polymorphism at the modifier loci. σ_γ is given by $\sqrt{\sum \mathrm{Var}(\gamma_i)}$, and is nonzero if one or more modifier loci are polymorphic. In the simulations, the number of loci with a significant contribution to the trait (i.e., with nonzero effect) increases with f (leading to a greater number of coexisting phenotypes; see Fig. 5), but the resulting genetic architecture is always asymmetric. Typically, the ratio of the effect of a locus to the effect of the next stronger locus is approximately 1:2. Polymorphism at the modifier loci increases with f and decreases with n. Especially for $n = 2$, alternative evolutionary outcomes are possible. Note that the scale of the horizontal axis is linear for $f \leq 10$ but logarithmic for $f \geq 10$. For $n = 4$ and $n = 5$, the symbols are slightly shifted to the right to increase visibility. The number of coexisting alleles per modifier locus, k, was limited to 20 for $n = 1$, eight for $n = 2$, six for $n = 3$, four for $n = 4$, and three for $n = 5$. $f = a/s$ with $s = 0.1$.

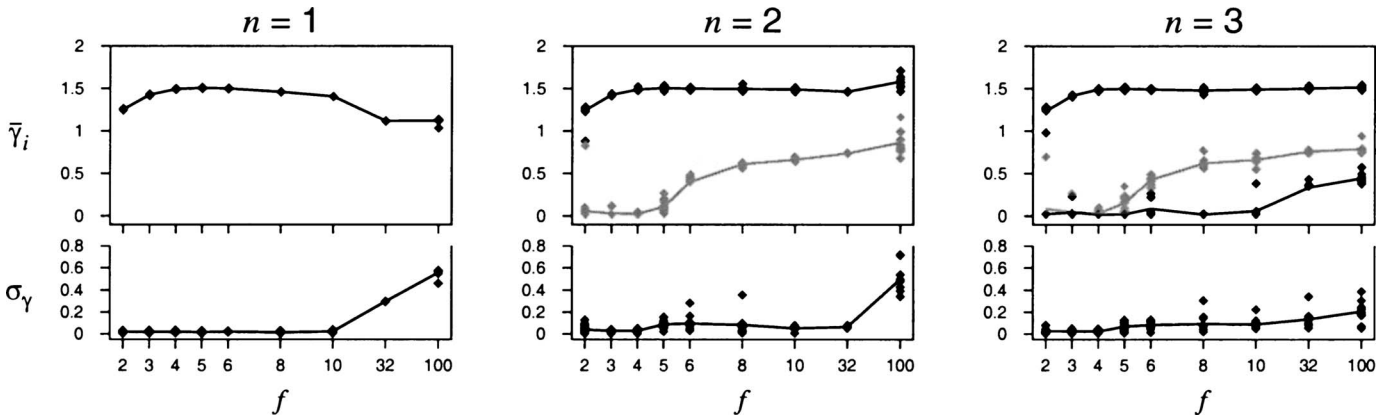

FIG. 7. The genetic architecture evolving in the diploid full model (eq. 5). Results are similar to the haploid model. See Figure 6 for more details. The number of coexisting alleles per modifier locus, k, was limited to 20 for $n = 1$, four for $n = 2$, and three for $n = 3$.

effects) increases with f and decreases with n. Second, the number of loci contributing to the trait increases with f, but the effect of each additional locus decreases exponentially (i.e., the ratio of locus effects is approximately 1:2:4:. . .). In consequence, the genetic architecture evolving under frequency-dependent disruptive selection is highly asymmetric, and even for very strong frequency dependence, the number of (polymorphic) loci with a significant effect on the phenotype is small.

The above results can be understood by noting two basic facts. First, let the number of loci with a mean effect significantly different from zero be denoted by $\tilde{n}$. Then, a haploid population with a ratio of locus effects equal to 1:2:. . . $2^{\tilde{n}-1}$ consists of $2^{\tilde{n}}$ equally spaced phenotypes. For example, for $n = \tilde{n} = 3$, $\gamma_1 = 1$, $\gamma_2 = 2$, and $\gamma_4 = 4$, these phenotypes are -7, -5, -3, -1, 1, 3, 5, and 7. Furthermore, if the allele frequencies at all primary loci are equal to 0.5 all phenotypes have the same frequency $1/2^{\tilde{n}}$. Second, this scheme is still somewhat inflexible, because the number of phenotypes can only be 2, 4, 8, 16, et cetera. More flexibility can be achieved with polymorphic modifiers. Indeed, one primary locus with an appropriate distribution of modifier alleles can produce any distribution of phenotypes. Sometimes, as for the case $f = 5$ in Figure 5, adding an additional major locus or an additional modifier allele are alternative solutions to the same problem. In other cases, especially when the number of primary loci is limited (most extremely, for $n = 1$), polymorphism at a modifier locus is the only possible solution. Figure 6 suggests that a ratio of locus effects of 1:2:4: . . . forms the backbone of the genetic architecture and that polymorphic modifier loci are added to fine-tune the phenotypic distribution. A potential explanation for this finding is that parallel evolution of multiple locus effects is faster than repeated evolutionary branching of a single locus effect.

An asymmetric genetic architecture evolves also in the diploid model (Fig. 7). Due to computational limitations, we could only test the one-, two-, and three-locus cases (with $\theta = 0$ and $r = 0.5$). However, the results are remarkably similar to those in the haploid case (Fig. 6). In particular, the number of loci contributing to the trait increases with f, and for high f, the ratio of locus effects is approximately 1:2 or 1:2:4 (for $n = 2$ or $n = 3$, respectively). Note that, in the diploid case, a genetic architecture with these locus effects produces equally spaced phenotypes, but in contrast to the haploid case, these phenotypes are not equally frequent. Polymorphism of modifier loci is weaker in the diploid model than in the haploid model, probably because the number of phenotypes is greater even with monomorphic modifiers.

In all cases, the total population size increases with the degree of frequency dependence, that is, with the number niches. The size of a haploid sexual population with an evolved genetic architecture is close to the size of an asexual population with the optimal phenotypic distribution. The size of a diploid sexual population is slightly lower (Fig. 8). It should be noted, however, that the phenotypic distribution in the asexual model does not maximize population size, and that there are many evolutionary unstable phenotypic distributions with similar equilibrium sizes (results not shown).

Finally, it should be noted that evolution of the genetic architecture is reasonably fast. With biologically realistic mutational parameters (see online Appendix 2), the pattern shown in Figures 6 and 7 is clearly visible after 5000 generations and stabilizes after about 30,000 to 40,000 generations (results not shown).

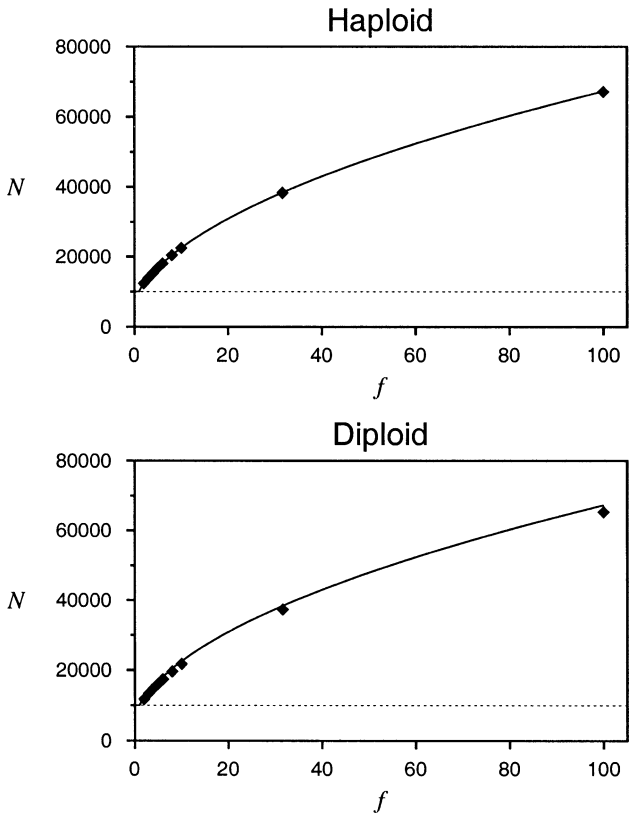

FIG. 8. Comparison of the population sizes in the asexual (solid line) and sexual versions (diamonds) of the full model (eq. 5) as a function of f, the degree of frequency dependence. The dotted line marks the carrying capacity for a phenotypically monomorphic population with $g = \theta$. In all models, population size increases with f. In the haploid sexual model, it is practically identical to the one in the asexual model. In the diploid sexual model, it is slightly lower. The values for the sexual models are means from the 10 replicates shown for $n = 5$ in Figure 6 (haploid) and for $n = 3$ in Figure 7 (diploid). Standard errors are too small to be visible at this scale.

DISCUSSION

We used a model of intraspecific competition and stabilizing selection to study how the genetic architecture (i.e., the distribution of locus effects) of a quantitative trait evolves under frequency-dependent disruptive selection. Our main result is twofold. First, frequency-dependent disruptive selection favors the evolution of a highly asymmetric genetic architecture. That is, if the genetic architecture can evolve freely and for a sufficiently long time, the trait and its genetic variance will be determined by a small number of loci, or even by a single major locus. The latter outcome occurs if frequency dependence (i.e., the relative strength of competition over stabilizing selection) is weak or if the phenotypic range of the trait is constrained. Second, these findings can be explained in terms of the niche structure created by intraspecific competition. Stable coexistence is possible only for a limited number of phenotypes, which increases with the

degree of frequency dependence. Evolution of the genetic architecture leads to a close match between this niche structure and the phenotypic distribution of a randomly mating population. As a consequence, a sexual population can reach almost the same size as an asexual one.

Evolution of Genetic Architecture as an Adaptation to Multiple Ecological Niches

Our results can be understood as follows. A phenotypic distribution that exactly matches the niche structure (and hence, is evolutionarily stable) can evolve easily only in an unconstrained asexual population. It cannot, in general, be attained by a randomly mating sexual population, because with a fixed genetic architecture, the phenotypic range is constrained and, additionally, segregation and recombination tend to create suboptimal intermediate phenotypes. However, the fit between the phenotypic distribution and the niche structure can be improved if the genetic architecture evolves. There are three factors contributing to this effect: (1) an adjustment of the phenotypic range of the trait eliminates overall disruptive selection; (2) a restriction of the number of loci contributing to the trait (possibly accompanied by polymorphism at modifier loci) matches the number of phenotypes to the number of niches; and (3) fine-tuning of the locus effects to match the phenotypes to the niches. With more than two or three niches, the ratio of locus effects is about 1:2:4: . . . , which results from the fact that the niches created by competition are approximately equally spaced.

In the haploid case, the match between the phenotypic distribution and the niche structure is perfect for two niches. If there are more than two niches, we still obtain a close match in the majority of simulations (Fig. 5). The asymmetric distribution of locus effects evolves also in the diploid case, even though segregation tends to produce heterozygotes with potentially maladaptive intermediate phenotypes. We expect that the niche structure would be matched more closely if we allowed for the evolution of dominance (van Dooren 1999; van Doorn 2004).

Generality of Results

For the extremely asymmetric genetic architectures shown in Figures 6 and 7 to evolve, we need to assume that one or two loci are indeed capable to cover the entire phenotypic range. If the maximal effect of a single primary locus is constrained, several polymorphic loci might be necessary to produce both extreme phenotypes (K. Schneider, unpubl. ms.). Even with this caveat, however, we still expect that frequency-dependent disruptive selection induces a trend toward an asymmetric distribution of locus effects and a reduction in the number of loci that contribute significantly to the trait variance. Indeed, several reasons make us believe that this trend is robust and general.

First, selection on the genetic architecture in our model is strong. As a consequence, for biologically realistic parameter values, a clearly asymmetric genetic architecture can evolve in fewer than 5000 generations. This situation is very different from the evolution of modifiers for background features such as mutation or recombination rates. Such modifiers have no direct effect on the phenotype and are under much weaker selection than trait loci. In contrast, selection on our modifiers is a first-order process.

Second, the ingredients of our model are very general. The weak-selection approximation (6) is an approximation not only of the Bulmer (1974) model but of all related competition models previously analyzed in the literature (Bürger 2005). Similarly, we allow for arbitrary symmetric effects of modifier alleles (see eq. 13, 14, and A16). Our simulations show that the predictions from the weak-selection approximation are qualitatively similar to those of the full model (eq. 5), as long as the latter gives rise to no more than two niches (i.e., as long as frequency dependence is relatively weak). With stronger frequency dependence, the Bulmer model (unlike the frequently used Roughgarden [1972] model; cf. Gyllenberg and Meszéna 2005; Polechová and Barton 2005) shows a structure of ecological niches that is likely to be generic for models of intraspecific competition. The existence of a finite number of discrete niches is in accordance with the principles of competitive exclusion and limiting similarity (e.g., Meszéna et al. 2006). A pattern similar to the one shown in Figure 4 has also been found in a model by Polechová and Barton (2005). Furthermore, our results seem to be qualitatively independent of population regulation. Patterns similar to the ones shown in Figures 4 and 6 can also be found if population size is held constant (unpubl. simulations). Finally, regimes of frequency-dependent disruptive selection are generic, in the sense that they can be evolutionary attractors (Geritz et al. 1998). This holds true not only for populations experiencing intraspecific competition, but also in a variety of other ecological scenarios, such as predation (Abrams and Matsuda 1997; Doebeli and Dieckmann 2000) or adaptation to heterogeneous environments (Geritz et al. 1998).

Indeed, several models of selection in spatially variable environments have produced results that are compatible with ours. All of these models are based on the two-niche case of Levene's (1953) soft-selection model. To our knowledge, the first study that explicitly considers the evolution of genetic architecture under frequency-dependent disruptive selection was van Dooren's (1999) model on the evolution of dominance. In agreement with our results, he found that evolution of the genetic architecture can increase the fit between a population's phenotypic distribution and the niche structure (in his case, by preventing heterozygotes from having a low-fitness intermediate phenotype). Several other results for Levene-type models can be understood in the same context. Kisdi and Geritz (1999a) and van Doorn (2004) used a continuum-of-alleles model, where the primary loci can have an infinite number of possible alleles. Invasion of a new primary locus allele into the population has an effect similar to the invasion of a new modifier allele in our model. Kisdi and Geritz (1999a) showed that alleles at a single locus can evolve to match the optimal phenotypes selected for in two different habitats. Their model was extended to a multilocus trait by van Doorn (2004), who found that genetic variation tends to accumulate at a single locus. Based on our results, we expect that more than one locus would remain polymorphic in a model with more than two habitats.

Despite theoretical arguments for its importance, good examples for frequency-dependent disruptive selection in na-

ture are still sparse. Recent analyses suggest that (pure) disruptive selection might be more common than previously thought (Kingsolver et al. 2001), but direct evidence for a combination of disruptive and frequency-dependent selection within a single species is only now starting to emerge (Bolnick et al. 2003; Swanson et al. 2003; Bolnick 2004). To our knowledge, there are no data showing if and how the genetic architecture of traits under frequency-dependent disruptive selection actually evolves. Hence, a rigorous empirical test of our predictions is not possible at this time.

However, frequency-dependent disruptive selection (due to intraspecific competition) is likely to be involved in the origin and maintenance of resource use polymorphisms (Smith and Skúlason 1996). A compelling example for a polymorphism that might be the end product of an evolving genetic architecture is provided by the African finch *Pyrenestes ostrinus* (Smith 1993). In this species, there are two randomly mating morphs that differ in beak size and are specialized on hard and soft seeds, respectively. The phenotypes of the two morphs coincide with fitness maxima. As predicted by our model for the two-niche case, the polymorphism is determined by a single locus (although, of course, beak size is a continuous trait that is influenced by many genes).

Implications

Implications for modelers

Our findings have several implications for models of traits under frequency-dependent disruptive selection. First, they once again show that genetic details are important for predicting the evolutionary trajectory. As demonstrated by Bürger (2005), the genetic architecture has a strong effect on the population-genetic equilibrium. In addition, we show that the genetic architecture is under strong selection. Therefore, neither the details of the genetic architecture nor the possibility of its evolution should be ignored. In particular, our results caution against the common assumption of a symmetric genetic architecture with equal locus effects (e.g., Dieckmann and Doebeli 1999; Nuismer et al. 2005; Bolnick 2006). Modelers should be aware that, together with an often arbitrary restriction of the phenotypic range, this assumption implies a strong constraint on the possible evolution of the trait. The same caveat applies to the so-called hypergeometric model (e.g., Shpak and Kondrashov 1999), which makes even stronger symmetry assumptions. At the very least, the effects of such symmetry assumptions should be tested by simulations (e.g., Bürger and Gimelfarb 2004; Bürger 2005). On the other hand, our results show that frequency-dependent disruptive selection does not necessarily maintain polymorphisms at a large number of loci (despite maintaining large phenotypic variances; see also van Doorn 2004). This lends some justification to models considering only one (Bulmer 1974; Christiansen and Loeschke 1980) or two (Loeschke and Christiansen 1984; Bürger 2002) polymorphic loci.

Implications for populations under frequency-dependent disruptive selection

Our results suggest a possible evolutionary pathway toward discrete polymorphisms, for example, with respect to resource use (Smith and Skúlason 1996). We show how a discrete polymorphism based on one or two loci can evolve from a more continuous phenotypic distribution determined by many loci (see also van Doorn 2004). Furthermore, we show that such a polymorphism can evolve through several intermediate steps, and that the phenotypes determined by a polymorphic locus can be fine-tuned via evolution of epistatically linked loci in the genetic background. For example, the two morphs of *P. ostrinus* coincide with fitness maxima (Smith 1993). It seems unlikely that this optimal state was achieved by a single mutation. More likely, after the primary polymorphism appeared, the two phenotypes have been adjusted by additional substitutions, either at the trait locus itself or in the genetic background.

More generally, our analysis suggests that evolution of the genetic architecture is a plausible way for populations to respond to frequency-dependent disruptive selection. Therefore, it is an alternative to other evolutionary responses, such as phenotypic plasticity, reduced migration rate (Kisdi and Geritz 1999b), sexual dimorphism (Bolnick and Doebeli 2003; van Dooren et al. 2004), or sympatric speciation (Dieckmann and Doebeli 1999; Doebeli and Dieckmann 2000). These other mechanisms can evolve because a fixed genetic architecture constrains the phenotypic distribution of a randomly mating population. Our results show that adaptation of the genetic architecture can make more complicated solutions unnecessary. This is particularly true for cases with only two niches, where a haploid population (or a diploid population with dominance) can exactly match the niche structure. Obviously, when there are several alternative evolutionary possibilities, the outcome of evolution will depend on many factors, including trade-offs, constraints, or initial conditions. Little is known about these factors, because most studies focus on a single possibility (but see Bolnick and Doebeli 2003; van Dooren et al. 2004).

Implications for the Evolution of Genetic Architecture

Our model treats an ecological scenario in which selection on the genetic architecture is much stronger than in previously studied cases. Most studies so far have focused on populations under stabilizing selection and in mutation-selection balance. The most famous example is Fisher's theory for the evolution of dominance (Fisher 1930; see also Mayo and Bürger 1997). In such systems, selection on dominance modifiers is very weak, because it is proportional to the frequency of a deleterious allele. Evolution of the genetic architecture is more likely in multilocus systems, where a single modifier can affect many loci (Wagner et al. 1997). Still, the strength of selection is limited by the mutation load (Hermisson and Wagner 2005; Proulx and Phillips 2005). Therefore, significant selection for evolution of genetic architecture can only be expected in traits influenced by a large number of loci or if the mutation rate is high (Visser et al. 2003). In stark contrast to these results, frequency-dependent disruptive selection maintains large genetic and phenotypic variances. Segregation and recombination can produce considerably maladaptive phenotypes, which provides ample opportunity (Proulx and Phillips 2005) for selection to adjust the genetic architecture.

Our results can also be interpreted in terms of genetic canalization (Waddington 1942; for a recent review, see Flatt 2005). The evolution of an asymmetric genetic architecture can be explained by noting that, once the phenotypic range is large enough, selection is no longer disruptive, but instead stabilizing for several phenotypes simultaneously. Stabilizing selection typically favors canalization. In other words, once a sufficient number of loci has evolved to generate the phenotypes corresponding to the ecological niches, the remaining polymorphic loci are canalized (i.e., their effect decreases) to reduce segregation and recombination load.

Finally, it is interesting to note that a trend toward the evolution of an asymmetric genetic architecture is also observed in models of stabilizing (Hermisson et al. 2003) and directional (Carter et al. 2005) selection. These studies, together with the present paper, suggest that such a trend could be a robust theoretical prediction. Empirically, the genetic architecture of quantitative traits is still poorly understood (reviewed by Mackay 2001; Barton and Keightley 2002; Bürger 2005, pp. 260–263). However, many (though by no means all) studies are, indeed, compatible with an asymmetric genetic architecture, where a trait is determined by a small number of major loci with strong effects plus a potentially large number of minor loci with very weak effects (Robertson 1967; Mackay 2001). Although it is unclear yet to what extent genetic architectures are adaptive, the available data are certainly in line with theoretical predictions.

Acknowledgments

We thank R. Bürger, T. Hansen, and an anonymous reviewer for helpful comments on the manuscript. This study was supported by an Emmy-Noether grant from the Deutsche Forschungsgemeinschaft to JH.

Literature Cited

Abrams, P. A., and H. Matsuda. 1997. Fitness minimization and dynamic instability as a consequence of predator-prey coevolution. Evol. Ecol. 11:1–20.

Abrams, P. A., H. Matsuda, and Y. Harada. 1993. Evolutionarily unstable fitness maxima and stable fitness minima of continuous traits. Evol. Ecol. 7:465–487.

Ackermann, M., and M. Doebeli. 2004. Evolution of niche width and adaptive dynamics. Evolution 58:2599–2612.

Barton, N. H., and P. D. Keightley. 2002. Understanding quantitative genetic variation. Nat. Rev. Genet. 3:11–21.

Bolnick, D. I. 2004. Can intraspecific competition drive disruptive selection? An experimental test in natural populations of sticklebacks. Evolution 58:608–613.

———. 2006. Multi-species outcomes in a common model of sympatric speciation. J. Theor. Biol. 241:734–744.

Bolnick, D. I., and M. Doebeli. 2003. Sexual dimorphism and adaptive speciation: two sides of the same ecological coin. Evolution 57:2433–2449.

Bolnick, D. I., R. Svanbäck, J. A. Fordyce, L. H. Yang, J. M. Davis, C. D. Husley, and M. L. Forister. 2003. The ecology of individuals: incidence and implications of individual specialization. Am. Nat. 161:1–28.

Brown, C. S., and T. L. Vincent. 1987. Coevolution as an evolutionary game. Evolution 41:66–79.

Bulmer, M. G. 1974. Density-dependent selection and character displacement. Am. Nat. 108:45–58.

Bürger, R. 2002. On a genetic model of intraspecific competition and stabilizing selection. Am. Nat. 160:661–682.

———. 2005. A multilocus analysis of intraspecific competition and stabilizing selection on a quantitative trait. J. Math. Biol. 50:355–396.

Bürger, R., and A. Gimelfarb. 2004. The effects of intraspecific competition and stabilizing selection on a polygenic trait. Genetics 167:1425–1443.

Bürger, R., and K. Schneider. 2006. Intraspecific competitive divergence and convergence under assortative mating. Am. Nat. 167:190–205.

Carter, A. J. R., J. Hermisson, and T. F. Hansen. 2005. The role of epistatic gene interactions in the response to selection and the evolution of evolvability. Theor. Popul. Biol. 68:179–196.

Christiansen, F. B., and V. Loeschke. 1980. Evolution and intraspecific exploitative competition. I. One-locus theory for small additive gene effects. Theor. Popul. Biol. 18:297–313.

Dieckmann, U., and M. Doebeli. 1999. On the origin of species by sympatric speciation. Nature 400:354–357.

Doebeli, M., and U. Dieckmann. 2000. Evolutionary branching and sympatric speciation caused by different types of ecological interactions. Am. Nat. 156:S77–S101.

Fisher, R. A. 1930. The genetical theory of natural selection. Clarendon Press, Oxford, U.K.

Flatt, T. 2005. The evolutionary genetics of canalization. Q. Rev. Biol. 80:287–316.

Gavrilets, S. 2004. Fitness landscapes and the origin of species. Princeton Univ. Press, Princeton, NJ.

Gavrilets, S., and D. Waxman. 2002. Sympatric speciation by sexual conflict. Proc. Natl. Acad. Sci. USA 99:10533–10538.

Geritz, S. A., E. Kisdi, G. Meszéna, and J. Metz. 1998. Evolutionary singular strategies and the adaptive growth and branching of the evolutionary tree. Evol. Ecol. 12:35–57.

Gyllenberg, M., and G. Meszéna. 2005. On the impossibility of coexistence of infinitely many strategies. J. Math. Biol. 50: 133–160.

Hansen, T. F. 2006. The evolution of genetic architecture. Annu. Rev. Ecol. Syst. 37:*in press*.

Hermisson, J., and G. P. Wagner. 2005. Evolution of phenotypic robustness. Pp. 47–69 *in* E. Jen, ed. Robust design: a repertoire from biology, ecology, and engineering. Oxford Univ. Press, Oxford, U.K.

Hermisson, J., T. F. Hansen, and G. P. Wagner. 2003. Epistasis in polygenic traits and the evolution of genetic architecture under stabilizing selection. Am. Nat. 161:708–734.

Kingsolver, J. G., H. Hoekstra, H. Hoekstra, D. Berrigan, S. Vignieri, C. Hill, A. Hoang, P. Gibert, and P. Beerli. 2001. The strength of phenotypic selection in natural populations. Am. Nat. 157:245–261.

Kisdi, E., and S. A. H. Geritz. 1999a. Adaptive dynamics in allele space: evolution of genetic polymorphism by small mutations in a heterogeneous environment. Evolution 53:993–1008.

———. 1999b. Evolutionary dynamics and sympatric speciation in diploid populations. Interim Report IR-99-048. International Institute for Applied System Analysis, Vienna, Austria.

Levene, H. 1953. Genetic equilibrium when more than one ecological niche is available. Am. Nat. 87:331–333.

Loeschke, V., and F. B. Christiansen. 1984. Evolution and intraspecific exploitative competition. II. A two-locus model for additive gene effects. Theor. Popul. Biol. 26:228–264.

Mackay, T. F. C. 2001. The genetic architecture of quantitative traits. Annu. Rev. Ecol. Syst. 35:303–339.

Mayo, O., and R. Bürger. 1997. The evolution of dominance: A theory whose time has passed? Biol. Rev. 72:97–110.

Meszéna, G., M. Gyllenberg, L. Pásztor, and J. A. J. Metz. 2006. Competitive exclusion and limiting similarity: a unified theory. Theor. Popul. Biol. 69:68–87.

Nuismer, S., M. Doebeli, and D. Browning. 2005. The coevolutionary dynamics of antagonistic interactions mediated by quantitative traits with evolving variances. Evolution 59:2073–2082.

Polechová, J., and N. H. Barton. 2005. Speciation through competition: a critical review. Evolution 59:1194–1210.

Proulx, S. P., and P. C. Phillips. 2005. The opportunity for canalization and the evolution of genetic networks. Am. Nat. 165: 147–162.

Robertson, A. 1967. The nature of quantitative genetic variation.

Pp. 265–280 *in* A. Brink, ed. Heritage from Mendel. Univ. of Wisconsin Press, Madison, WI.
Roughgarden, J. 1972. Evolution of niche width. Am. Nat. 106: 683–718.
Shpak, M., and A. S. Kondrashov. 1999. Applicability of the hypergeometric phenotypic model to haploid and diploid populations. Evolution 53:600–604.
Smith, T. B. 1993. Disruptive selection and the genetic basis of bill size polymorphism in the African finch *Pyrenestes*. Nature 363: 618–620.
Smith, T. B., and S. Skúlason. 1996. Evolutionary significance of resource polymorphisms in fishes, amphibians, and birds. Annu. Rev. Ecol. Syst. 27:111–133.
Swanson, B. O., A. C. Gibb, J. C. Marks, and D. A. Hendrickson. 2003. Trophic polymorphism and behavioral differences decrease intraspecific competition in a cichlid, *Herichthys minckleyi*. Ecology 84:1441–1446.
van Dooren, T. J. M. 1999. The evolutionary ecology of dominance-recessivity. J. Theor. Biol. 198:519–532.
van Dooren, T. J. M., M. Durinx, and I. Demon. 2004. Sexual dimorphism or evolutionary branching? Evol. Ecol. Res. 6: 857–871.
van Doorn, G. S. 2004. Sexual selection and sympatric speciation. Ph.D. diss., Groningen University, Groningen, The Netherlands.
Visser, J. A. G. M., J. Hermisson, G. P. Wagner, L. A. Meyers, H. Bagheri-Chaichian, J. L. Blanchard, L. Chao, J. M. Cheverud, S. F. Elena, W. Fontana, G. Gibson, T. F. Hansen, D. Krakauer, R. C. Lewontin, C. Ofria, S. H. Rice, G. von Dassow, A. Wagner, and M. C. Whitlock. 2003. Perspective: evolution and detection of genetic robustness. Evolution 57:1959–1972.
Waddington, C. H. 1942. Canalization of development and the inheritance of acquired characters. Nature 150:563–565.
Wagner, G. P., G. Booth, and H. Bagheri-Chaichian. 1997. A population genetic theory of canalization. Evolution 51:329–347.

Corresponding Editor: T. Hansen

Appendix 1: Analytical Results for the Weak-Selection Approximation

In the following, we provide additional details regarding the analytical results presented in the main text. In order to treat the haploid and diploid case within the same framework, we introduce the parameter

$$\tau = \begin{cases} 1 & \text{in the haploid case} \\ 2 & \text{in the diploid case.} \end{cases} \tag{A1}$$

Evolutionary Equilibrium with Fixed Genetic Architecture for Constant Population Size at Linkage Equilibrium

Here, we briefly review important results of Bürger (2005) and Bürger and Schneider (2006), which we use in the derivation of our analytical results.

The variable Θ_m in inequalities (10) is given by

$$\Theta_m \equiv \tau \frac{\theta - \delta_\theta \sum_{i=1}^{m} \gamma_i}{\tau(n - m) + \eta - 1}, \tag{A2}$$

with $\delta_\theta \equiv \text{sign}(\theta)$. Note that

$$\text{sign}(\Theta_m) = \delta_\theta. \tag{A3}$$

For monomorphic loci, the frequency of the A_i allele is

$$p_i = \begin{cases} 0 & \text{if } \theta < 0 \\ 1 & \text{if } \theta > 0. \end{cases} \tag{A4a}$$

If $\theta = 0$ or if all loci have identical effects γ_i, then there are no monomorphic loci. For polymorphic loci, the frequency of the A_i allele is

$$p_i = \frac{1}{2} + \frac{\Theta_m}{2\gamma_i}. \tag{A4b}$$

Thus, the deviation of the allele frequency from the symmetric state $p_i = 1/2$ is inversely proportional to the locus effect γ_i, showing that the contribution of each polymorphic locus to the mean phenotype $\bar{g}$ equals Θ_m. It is worth noting that the monomorphic loci are exactly those loci that cannot make this contribution (because their $\gamma_i < |\Theta_m|$). Furthermore, at equilibrium, the mean phenotype is

$$\bar{g} = \frac{1 - \eta}{\tau}\Theta_m + \theta, \tag{A5}$$

which implies, in particular, that $\bar{g}$ is always between zero and the optimal phenotype θ, and the phenotypic variance is

$$V = \frac{1}{\tau} \sum_{i>m} [\gamma_i^2 - (\Theta_m)^2], \tag{A6}$$

which shows that strong loci contribute most to V.

Derivation of the Invasion Fitness Gradients

In this section, we derive the selection gradients given in equation (12). Let p_i and q_i denote the frequencies at locus i of the A_i and a_i allele, respectively. Then the mean phenotype of a population with an homogeneous genetic architecture is

$$\bar{g} = \sum_{i=1}^{n} (p_i - q_i)\gamma_i, \tag{A7}$$

and the phenotypic variance at linkage equilibrium is

$$V = \frac{4}{\tau} \sum_{i=1}^{n} p_i q_i \gamma_i^2. \tag{A8}$$

Furthermore, equation (6) can be rearranged to

$$W(g) = \omega_0 + \omega_1 g + \omega_2 g^2, \tag{A9}$$

with

$$\omega_0 = 1 - s\theta^2 + s\eta(\bar{g}^2 + V), \tag{A10a}$$

$$\omega_1 = 2s(\theta - \eta\bar{g}), \quad \text{and} \tag{A10b}$$

$$\omega_2 = s(\eta - 1) \tag{A10c}$$

(cf. Bürger 2005). The mean fitness of individuals carrying a copy of the mutant modifier allele is given by

$$\begin{aligned} \bar{W}^* &= \omega_0 + \omega_1 \bar{g}^* + \omega_2 \text{E}[(g^*)^2] \\ &= \omega_0 + \omega_1 \bar{g}^* + \omega_2 [V^* + (\bar{g}^*)^2], \end{aligned} \tag{A11}$$

where E denotes the expectation and $\bar{g}^*$ and V^* are the phenotypic mean and variance of the mutants. In the terminology of adaptive dynamics, $\bar{W}^*$ is the invasion fitness.

As, for a rare mutation, the ω values do not depend on the mutant parameters, the selection gradients evaluate to

$$\frac{\partial \bar{W}^*}{\partial \gamma_i^*} = (\omega_1 + 2\omega_2 \bar{g}^*) \frac{\partial \bar{g}^*}{\partial \gamma_i^*} + \omega_2 \frac{\partial V^*}{\partial \gamma_i^*}. \tag{A12}$$

The next task is to calculate the derivatives of the mutant phenotypic mean and variance with respect to the mutant locus parameters. As the modifier locus is assumed to be unlinked to the primary loci, $\bar{g}^*$ and V^* are obtained from equations (A7) and (A8) by inserting the mutant locus effect γ_i but the resident allele frequencies p_j and q_j (which are independent of the mutation). Using equations (A7) and (A8), it is straightforward to see that these are

$$\frac{\partial \bar{g}^*}{\partial \gamma_i^*} = p_i - q_i \quad \text{and} \tag{A13a}$$

$$\frac{\partial V^*}{\partial \gamma_i^*} = \frac{8}{\tau} p_i q_i (\gamma_i^*)^2. \tag{A13b}$$

Now we can plug equations (A13) into equations (A12) and evaluate the result at the point where the mutant and resident locus effects are equal ($\boldsymbol{\gamma}^* = \boldsymbol{\gamma}$). Noting that, due to (A10) and (A5), at this point

$$\varpi_1 + 2\varpi_2\bar{g} = 2s(\theta - \bar{g}) = \frac{2}{\tau}s(\eta - 1)\Theta_m, \tag{A14}$$

it is straightforward to arrive at equation (12a) with

$$Q_i = \Theta_m(p_i - q_i) + 4p_iq_i\gamma_i, \tag{A15}$$

which evaluates to (12b), using (A4a) and (A3) for $i \leq m$ and $p_i - q_i = \Theta_m/\gamma_i$ and $4p_iq_i\gamma_i = \gamma_i - \Theta_m^2/\gamma_i$ (from A4b) for $i > m$.

Proof that Phenotypic Variance Is Maximized under Symmetric Stabilizing Selection

Rewriting equation (15) in integral form (and neglecting the constant $s[\eta - 1]/\tau$) yields

$$\Omega = \sum_i \int 2Q_i \, d\gamma_i$$

$$= \left[\tau\frac{2|\theta| - \delta_\theta\Gamma_m}{\tau(n - m) + \eta - 1}\right]\sum_{i\leq m}\gamma_i + \sum_{i>m}\gamma_i^2, \tag{A16}$$

with $\Gamma_m = \Sigma_{i\leq m}\gamma_i$. (Note that, in contrast to the previous derivations, Θ_m is not treated as a constant in the integration.) As $\boldsymbol{\gamma}$ evolves, Ω always increases. For $\theta = 0$, Ω equals V, which shows that evolution of the genetic architecture maximizes the phenotypic variance.

Proofs of the Conclusions for the Model with Constant Γ

Here, we proof the conclusions reached from equation (19) for the case $\Gamma \to \Gamma_{max}$. We will use the fact that, due to (8), (10), and (12b),

$$Q_1 = \cdots = Q_m < Q_{m+1} \leq \cdots \leq Q_n. \tag{A17}$$

(1) The strongest locus always increases in strength:

$$\tilde{Q}_c = \sum_i Q_i\gamma_i < Q_n\sum_i \gamma_i = \gamma_n\Gamma_{max}. \tag{A18}$$

(2) The weakest locus always decreases in strength:

$$\tilde{Q}_c = \sum_i Q_i\gamma_i > Q_1\sum_i \gamma_i = \gamma_i\Gamma_{max}. \tag{A19}$$

(3) All monomorphic loci decrease in strength:

$$\tilde{Q}_c = \sum_i Q_i\gamma_i > Q_{i\leq m}\sum_i \gamma_i = Q_{i\leq m}\Gamma_{max}. \tag{A20}$$

(4) At the long-term equilibrium, the genetic architecture is characterized by a single major locus ($\gamma_n = \Gamma_{max}$, $\gamma_i = 0$ for $i < n$): using equation (A16), the long-term equilibrium of $\boldsymbol{\gamma}$ can be found by maximizing Ω with respect to the γ_i under the boundary condition $\Sigma_i\gamma_i = \Gamma_{max}$. Clearly, the first term in equation (A16) decreases with η. Therefore, it is sufficient to consider the case $\eta \to 1$. Furthermore, for fixed Γ_m, the second term in (A16) is maximal if there is a single polymorphic locus with effect $\gamma_n = \Gamma_{max} - \Gamma_m$. Thus, it is sufficient to consider the case $m = n - 1$. The right side of equation (A16) then evaluates to $(2|\theta| - \Gamma_m)\Gamma_m + (\Gamma_{max} - \Gamma_m)^2 = \Gamma_{max} - 2\Gamma_m(\Gamma_{max} - |\theta|)$, which is maximal for $\Gamma_m \to 0$ (because we assume $|\theta| < \Gamma_{max}$). This completes the proof.

Online Appendices to "The Evolution of Genetic Architeture under Frequency-dependent Disruptive Selection"

Michael Kopp Joachim Hermisson

Appendix 2: Simulations

In this Appendix, we describe the numerical simulations.

General procedure.— We used deterministic simulations of haplotype frequencies, coupled with stochastic creation and extinction of modifier alleles. A haplotype is defined by the allelic values at both the primary and modifier loci, with the alleles at the modifier loci determining the mutational effects of the primary loci. We assume one modifier locus per primary locus. In principal, there are infinitely many modifier alleles and, therefore, infinitely many haplotypes. In order to keep the number of haplotypes finite we only allow a fixed number k of alleles per modifier locus to be simultaneously present in the population (between 2 and 20, depending on the number of loci).

Our simulated haplotypes undergo a repeated sequence of selection, segregation (in the diploid case), recombination, and mutation. More precisely, for each genotype, we first calculate the phenotype g, and then apply equation (5) or (6) to obtain the corresponding fitness values. To get haplotype frequencies after selection and recombination, we use the standard recursion relation

$$p'_r = \bar{W}^{-1} \sum_{s,t} W_s W_t p_s p_t R(st \to r) \tag{A21a}$$

in the haploid case and

$$p'_r = \bar{W}^{-1} \sum_{s,t} W_{st} p_s p_t R(st \to r) \tag{A21b}$$

in the diploid case. Here, haplotypes are labeled r, s, and t, and p_r and p'_r are the haplotype frequencies before and after selection and recombination, respectively. W_x is the fitness of a haploid individual with genotype x, and W_{xy} is the fitness of a diploid individual

containing haplotypes x and y. $R(st \to r)$ is the rate at which recombination events between haplotypes s and t produce haplotype r. The $R(st \to r)$'s are calculated from the recombination rates between pairs of adjacent loci, which are model parameters, and from the number of recombination events necessary to create the target genotype. Between each pair of adjacent loci, at most one recombination event can occur, and recombination events between different pairs of adjacent loci are assumed to be independent. Modifier loci are adjacent to their respective primary loci. Population sizes follow the recursion relation

$$N' = N\bar{W}. \tag{A22}$$

Mutation is handled differently for primary loci and modifier loci. Primary locus alleles mutate from A_i to a_i and vice versa at rate 10^{-5} per individual and generation. Their allele frequencies change deterministically according to this rate. In contrast, mutations at modifier loci are modeled stochastically. If, at a modifier locus, less than k alleles are present in the population, one of them can give rise to a new, mutant allele with probability 0.01 per generation (note that this probability refers to the whole population, not to each single individual). The allelic value of the mutant allele is drawn from a normal distribution with mean equal to the value of the source allele and variance V_m. Mutations leading to a negative value of γ_i are rejected. The initial frequency of the new allele is set to $10/\tau N$, corresponding to 10 initial copies in the population. An allele of this frequency has a negligible chance of being lost due to genetic drift. In other words, we only consider alleles which have survived the initial threat of stochastic extinction. Once a modifier allele has entered the population, its subsequent dynamics are determined by the deterministic equations (A21). The only exception is extinction. A modifier allele with frequency μ can go extinct with probability $(1-\mu)^{\tau N}$, which is the probability that it is not present in any of the τN haplotypes of the next generation.

Technical assumptions.— As described above, the simulations are very time consuming. In order to increase computation speed, we made several technical assumptions:

First, the time required for the recombination step in equations (A21) is of order $O(z^3)$, where z is the number of possible haplotypes. In simulations with free recombination ($r = 0.5$), this can be reduced to $O(z)$ by making the simplifying assumption that recombination always restores complete linkage equilibrium. Therefore, in many simulations, instead of using equations (A21), we calculated haplotype frequencies after selection and mutation, used these to extract allele frequencies, and then calculated haplotype frequencies at linkage equilibrium as the products of the respective allele frequencies. We will refer to this simplification as the linkage equilibrium assumption.

Second, in the full model (eq. 5), the time required for the computation of $\bar{\alpha}_\pi(g)$ is of order $O(z^2)$ in the haploid case and $O(z^4)$ in the diploid case. These relationships can be reduced to $O(z)$ and $O(z^2)$, respectively, if on the right-hand side of equation (2b), the average is taken not over all possible phenotypes, but only over the means of 20 equally

spaced phenotypic classes (like those in a histogram). The effect of this simplification on the resulting fitness values is negligible.

Third, we did not allow mutations in modifier loci that resulted in γ_i values too similar to those of existing alleles. More precisely, mutant alleles with a distance less than $\sqrt{V_m}/4$ from a previously existing allele were assigned a value at exactly this distance from the existing allele. In cases where the new allele fell in between two previously existing alleles with distance less than $\sqrt{V_m}/2$, its distance from the nearer of the two existing alleles was set to 1/4 of the distance between them.

Fourth, instead of explicitly modeling mutations at primary loci, we only prevented allele frequencies from becoming less than 10^{-5}. This assumption has negligible effects provided selection on a locus is not extremely weak (i.e., unless the locus effect is very close to 0.)

The weak-selection approximation with constrained phenotypic range.— The assumptions about the mutation process laid down in equations (16) were implemented as follows: We introduce "internal" variables $\hat{\gamma}_i$ which are assumed to be directly coded for by the modifier loci (one per primary locus). The $\hat{\gamma}_i$ can evolve independently, but they interact epistatically to produce the locus effects γ_i, according to

$$\gamma_i = \phi(\hat{\Gamma})\frac{\hat{\gamma}_i}{\hat{\Gamma}} \tag{A23a}$$

with

$$\hat{\Gamma} = \sum_i \hat{\gamma}_i \tag{A23b}$$

and

$$\phi(\hat{\Gamma}) = \frac{\Gamma_{\max}\hat{\Gamma}}{\beta + \hat{\Gamma}}. \tag{A23c}$$

where $\beta > 0$. We always used $\Gamma_{\max} = 1$ and $\beta = 1$. Other fixed parameter values were: $k = 2$, $a = 0.2$, $V_m = 0.04$, $\rho = 2$, $\kappa = 10^4$.

For the case with free recombination, we investigated the following parameter combinations: weak versus strong frequency-dependence ($f = 2$ versus $f = 10$), symmetric versus asymmetric stabilizing selection ($\theta = 0$ versus $\theta = 0.5$), and haploid versus diploid genetics with 2, 3, or 4 primary loci. For the four-locus cases, we used the linkage equilibrium assumption. All simulations were started with equal locus effects (i.e., a symmetric genetic architecture): either $\hat{\gamma}_i = 0.01$ (leading to a population with low initial phenotypic variance) or $\hat{\gamma}_i = 4/(\tau n)$ (leading to a population with high initial phenotypic variance). In the latter case, the sum of initial (mean) locus effects, $\sum \bar{\gamma}_j = 0.8\Gamma_{\max}$. The simulations were stopped when the mean effect of the strongest locus alone exceeded $0.8\Gamma_{\max}$. (Note that, due to eq. (A23c), an effect of $1.0\Gamma_{\max}$ can be reached only asymptotically.) This

condition was always reached, and when it was reached, the mean effects of all other loci were always less than $0.11\Gamma_{\max}$ and in many cases, less than $0.01\Gamma_{\max}$. Simulations with linkage were done only for the haploid case. We tested a range of values of r (0.01, 0.02, 0.03, 0.04, 0.05, 0.075, and 0.1) for $n = 2$ with $\theta = 0$ or $\theta = 0.5$ and $f = 2$ or $f = 10$, and for $n = 2$ with $\theta = 0$ and $f = 10$. Figure 2 shows the results for $n = 3$, $\theta = 0$, and $f = 10$.

The full model.— In simulations of the full model (eq. 5), we assumed that the effect of each locus was determined exclusively by the allelic values at the corresponding modifier locus. We usually used the linkage equilibrium assumption. As described in the main text, linkage disequilibrium is negligible for $r > 0.05$. Most simulations (including the ones presented in the main text) were started with equal locus effects of $\gamma_i = 0.01$ (i.e., assuming a low initial phenotypic variance). In some limited simulations, the initial locus effects were higher, but generically, we found the same results as those presented in the main text.

An important conclusion from our simulations is that an asymmetric genetic architecture can evolve in a reasonably short time-span (less than 5000 generations). Of course, the rate of evolution depends strongly on the mutation rate and on the variance of mutational effects at the modifier loci. Regarding mutation rates, we assumed that new alleles can invade the population (without being immediately lost by drift) at a rate of 0.01 per generation. For comparison, according to standard theory, the rate of fixation of beneficial alleles under stabilizing selection is approximately $\tau NusV_m$, with u being the mutation rate. With N between 10^4 and 10^5 (Fig. 8), u between 10^{-4} and 10^{-5}, $s = 0.1$ and $V_m = 0.04$, this is quite exactly in the order of 10^{-2}. As we only allow new mutations when there are less than k resident alleles, the effective mutation rate in our simulations is clearly conservative. Regarding the variance of mutational effects, we usually used $V_m = 0.04$. This means that the width of the corresponding normal distribution is about a fifth of the width of the stabilizing selection function (for $s = 0.1$), which is well in line with empirical estimates reviewed by Bürger (2005, pp. 263-267). In all simulations, we assumed $\rho = 2$, $\kappa = 10^4$, and $s = 0.1$.

References

Bürger, R., 2005. A multilocus analysis of intraspecific competition and stabilizing selection on a quantitative trait. J. Math. Biol. 50:355–396.

Appendix 3: Analysis of the full model with asexual reproduction

The equilibrium phenotypic distribution in the asexual version of the full model (eq. 6) can be determined without considering explicit genetics. The task is to find a vector $\mathbf{g} = (g_1, \ldots, g_k)$ of k coexisting phenotypes that satisfy the following three conditions: First, each phenotype is at population-dynamic equilibrium; that is, $W(g_i) = 1$ for $i = 1 \ldots k$. This condition yields the equilibrium numbers $N_i = N\pi(g_i)$ of individuals with genotype g_i as solutions of a linear system of equations. Second, each phenotype corresponds to a fitness optimum, that is the selection gradient $\partial W(g_i)/\partial g_i = 0$ for $i = 1 \ldots k$. This condition can be solved numerically. Third, no other phenotype can invade the population; that is, $W(h) < 1$ for all h that are not elements of $\mathbf{g}$. This condition defines the number of phenotypes, k. In practical terms, the bifurcation points shown in Figure 4 can be computed exactly by making the conjecture (which can be supported numerically) that, with increasing f, additional phenotypes always appear at $g_{\text{new}} = \theta$: When there was previously no $g_i = \theta$, $g_{\text{new}} = \theta$ invades if $W(g = \theta) = 1$. If a $g_i = \theta$ exists, it bifurcates into two new phenotypes if the second derivative $\partial^2 W(g = \theta)/\partial g^2 = 0$, that is if the point $g = \theta$ turns from a fitness maximum to a fitness minimum.

Appendix 4: Analysis of the full model with asymmetric stabilizing selection and linkage

In the main text, we have only analyzed cases with symmetric stabilizing selection and free recombination. However, our main results – in particular, that of an asymmetric genetic architecture with a ratio of locus effects of about $1 : 2 : 4 \ldots$ – also hold true for more general conditions. With asymmetric stabilizing selection, typically one or more primary loci become fixed and the combined effect of these loci evolves to a value equal to the optimal phenotype θ. In consequence, the population mean phenotype equals θ, and selection on the effects of the remaining polymorphic loci is the same as in the symmetric case. The only exceptions occur if the number of primary loci, n, is small and f is large. In this case, there is a trade-off between fixing loci to shift to the right the mean phenotype towards the optimum and keeping all loci polymorphic to increase the number of phenotypes. Selection may then favor the latter option, leading to an asymmetric phenotypic distribution with allele frequencies at the primary loci being greater than 0.5 but the mean phenotype $\bar{g} < \theta$ (assuming $\theta > 0$; results not shown).

We also tested the effects of linkage on the outcome of evolution. Significant linkage disequilibrium builds up only if the recombination rate between adjacent loci, r, is less than about 0.05. In these cases, the genetic architecture is less asymmetric than in the cases with free recombination, but the overall pattern still holds true (results not shown).